

Observation of 40 keV Field-Aligned Ion Beams

20 December 1998

Prepared by

R. B. SHELDON and H. E. SPENCE
Boston University Center for Space Physics
Boston, MA

J. F. FENNELL
Space and Environment Technology Center
Technology Operations

Prepared for

SPACE AND MISSILE SYSTEMS CENTER
AIR FORCE MATERIEL COMMAND
2430 E. El Segundo Boulevard
Los Angeles Air Force Base, CA 90245

Engineering and Technology Group


19990316 006



This report was submitted by The Aerospace Corporation, El Segundo, CA 90245-4691, under Contract No. F04701-93-C-0094 with the Space and Missile Systems Center, 2430 E. El Segundo Blvd., Los Angeles Air Force Base, CA 90245. It was reviewed and approved for The Aerospace Corporation by A. B. Christensen, Principal Director, Space and Environment Technology Center. Peter Bissegger was the project officer for the Mission-Oriented Investigation and Experimentation (MOIE) program.

This report has been reviewed by the Public Affairs Office (PAS) and is releasable to the National Technical Information Service (NTIS). At NTIS, it will be available to the general public, including foreign nationals.

This technical report has been reviewed and is approved for publication. Publication of this report does not constitute Air Force approval of the report's findings or conclusions. It is published only for the exchange and stimulation of ideas.


Peter Bissegger
SMC/AXES

REPORT DOCUMENTATION PAGE			Form Approved OMB No. 0704-0188	
Public reporting burden for this collection of information is estimated to average 1 hour per response, including the time for reviewing instructions, searching existing data sources, gathering and maintaining the data needed, and completing and reviewing the collection of information. Send comments regarding this burden estimate or any other aspect of this collection of information, including suggestions for reducing this burden to Washington Headquarters Services, Directorate for Information Operations and Reports, 1215 Jefferson Davis Highway, Suite 1204, Arlington, VA 22202-4302, and to the Office of Management and Budget, Paperwork Reduction Project (0704-0188), Washington, DC 20503.				
1. AGENCY USE ONLY (Leave blank)		2. REPORT DATE 20 December 1998		3. REPORT TYPE AND DATES COVERED
4. TITLE AND SUBTITLE Observation of 40 keV Field-Aligned Ion Beams			5. FUNDING NUMBERS F04701-93-C-0094	
6. AUTHOR(S) R. B. Sheldon, H. E. Spence, and J. F. Fennell				
7. PERFORMING ORGANIZATION NAME(S) AND ADDRESS(ES) The Aerospace Corporation Technology Operations El Segundo, CA 90245-4691			8. PERFORMING ORGANIZATION REPORT NUMBER TR-99(8570)-11	
9. SPONSORING/MONITORING AGENCY NAME(S) AND ADDRESS(ES) Space and Missile Systems Center Air Force Materiel Command 2430 E. El Segundo Boulevard Los Angeles Air Force Base, CA 90245			10. SPONSORING/MONITORING AGENCY REPORT NUMBER SMC-TR-99-03	
11. SUPPLEMENTARY NOTES				
12a. DISTRIBUTION/AVAILABILITY STATEMENT Approved for public release; distribution unlimited			12b. DISTRIBUTION CODE	
13. ABSTRACT (Maximum 200 words) Recent observations by CEPPAD/IPS from the new perspective of the POLAR orbit reveal a close association of field-aligned ionospheric beams with convecting plasmasheet "nose" ions. April 15, 1996 was marked by a large southward BZ accompanying a fast solar wind shock. This event triggered a strong cross-tail convection electric field that pushed plasmasheet ions deep into the magnetosphere. When the POLAR spacecraft passed through the inner magnetosphere, it observed both an unusually energetic "nose" plasmasheet ion injection at ~90 keV, as well as a peculiar field-aligned beam at ~40 keV. These beams appear to be enriched in oxygen ions (as inferred from other instruments), which would place their origin in the ionosphere. Both populations existed from L = 7-3, for a duration of at least 2 h. We speculate that the nose ions create a parallel electric field that is responsible for the extended ionospheric beam signature.				
14. SUBJECT TERMS Energetic particles, Ions, Storms, Field aligned, Ion beams, Magnetosphere			15. NUMBER OF PAGES 5	
			16. PRICE CODE	
17. SECURITY CLASSIFICATION OF REPORT UNCLASSIFIED	18. SECURITY CLASSIFICATION OF THIS PAGE UNCLASSIFIED	19. SECURITY CLASSIFICATION OF ABSTRACT UNCLASSIFIED	20. LIMITATION OF ABSTRACT	

Acknowledgments

This study was supported at Boston University by NASA contract NAS5-30368 and NSF grant ATM-9458424. The work at Aerospace was supported in part by Air Force Contract No. F04701-93-C-0094 and Boston University contract GC 131165 NGD. The authors gratefully acknowledge K. Ogilvie, E. Shelley, J. Dudeney, G. Rostoker, B. Blake, and T. Fritz for the use of their data.

Contents

Data Analysis	1
Nose Ions	1
Field-Aligned Beam.....	3
Peak Fits	3
Discussion and Conclusions	4
References	5

Figures

1. POLAR/CEPPAD/IPS data on April 14, April 14–15, and April 15, 1996, displaying energy spectra summed over pitch angles from 20–1500 keV	1
2. POLAR/CEPPAD/IPS data on April 15, 1996, displaying roll modulation of the counts in the 90° head in the energy bands from 18–138 keV	1
3. April 14–15, 1996 ISTP data	2
4. Successive 96s count spectra and three peak fit for April 15 dataset, corresponding to vertical slice through the data of Figure 1b and Figure 2	4
5. Parameters from the peak fits of Figure 4	4

Data Analysis

The POLAR spacecraft is in a polar, $9 \times 2 R_E$ orbit that in April 1996, was in the noon-midnight meridian plane with perigee over the south pole, making diagonal passes through the midnight and noon radiation belts. The Comprehensive Energetic Particle and Pitch Angle Distribution experiment's Imaging Proton Spectrometer (CEPPAD/IPS) [Blake *et al.*, (1995)], consists of a multiple solid state detectors that measure ions between 15–1500 keV in 9 elevation angles and 32 or less azimuthal bins. Three consecutive passes through the ring current (RC) starting on April 14, 1996 are plotted (Figure 1), going from midnight to noon over the south polar cap essentially along the noon-midnight meridian. The MLT and L -shell vary slightly with each pass, but are unimportant for the gross characteristics discussed here. Panel (a) shows a typical pass with an energetic particle population whose average energy is proportional to the $|B|$ defining the RC, and with a dropout in the middle of each pass corresponding to the fast perigee pass over the south polar cap. It shows the adiabatic energization expected from Liouville's theorem, and the consequent formation of the RC as an equilibrium distribution for ions diffusing in L -shell from a source region in the plasmasheet [Sheldon and Gaffey (1993)],

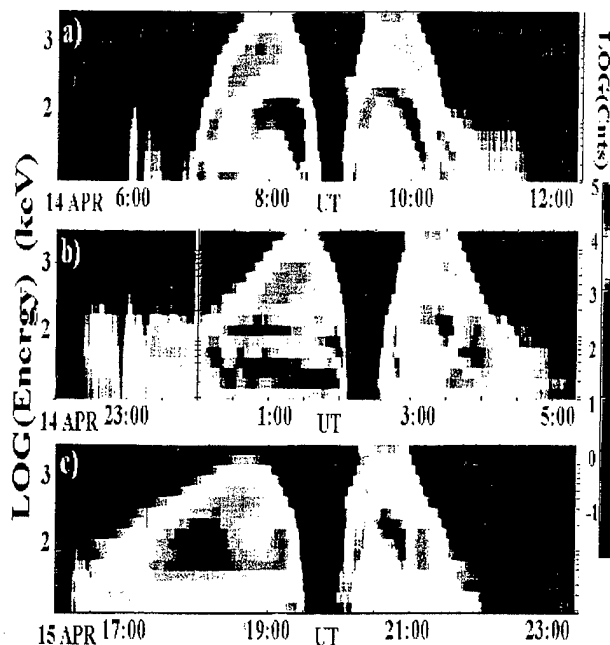


Figure 1. POLAR/CEPPAD/IPS data on (a) April 14, and (b) April 14-15, and (c) April 15, 1996, displaying energy spectra summed over pitch angles from 20–1500 keV.

On April 15, however, IPS detected two nearly monoenergetic bands superposed on the night side RC (panel b) at ~ 90 keV, and at ~ 40 keV. Unlike the RC, these two bands dropped to lower energies with lower L -shell, displaying an apparent non-adiabatic behavior. The bands became less distinct on the dayside and more sporadic, but apparently existed throughout the RC pass. On the following pass, we find no evidence for these bands other than a newly trapped energetic component of the RC. To better understand these ions, we examine only the lowest 8 energy channels and display the roll modulation as the spacecraft rotates with spin axis perpendicular to the magnetic field (Figure 2).

Nose Ions

We observed that the upper, ~ 90 keV band is strongly peaked around 90° and the lower band is peaked near 0° . This is reminiscent of “zipper” distributions observed nearly continuously at these L -shells by SCATHA [Fennell *et al.*, (1981)] and CRRES (H. Collin, private communication, 1997), though at ten times the energy of the earlier observations. A careful analysis of this event then, may shed light on the zipper mechanism that operates nearly continuously in the outer RC.

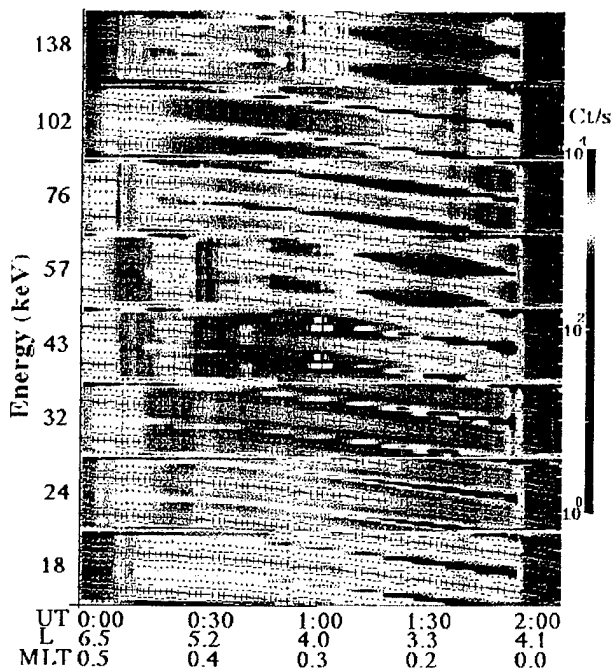


Figure 2. POLAR/CEPPAD/IPS data on April 15, 1996, displaying roll modulation of the counts in the 90° head in the energy bands from 18–138 keV. The (+), and (dots) are 90° and 30° pitchangles.

Now a monoenergetic trapped population is possible when a strong cross-tail electric field drives ions against the ∇B drift deep into the magnetosphere [Smith and Hoffman (1974)]. Such a "nose" event must be nearly 90° trapped particles because of the large increase in $|B|$ while convecting from the plasmasheet, a characteristic of the upper energy band in our data. These do not appear to be related to substorm injections, since examination of substorm injected ions shows them to be energy dispersed, as well as much more isotropic than these. With only these two options available, we identify our upper energy band with a nose event. Since nose events are highly correlated with storms, and storms are defined by D_{ST} , we turn to the preliminary D_{ST} provided by Kyoto University.

After subtracting the ionospheric S_Q contribution using the quietest day of the month, April 7–8, we find a moderate storm of at least -63 nT on the first hour of April 15. More significantly, we find a very large asymmetric H-component ($ASY = -200$ nT) on that day. Examination of the one-minute symmetric H-component (D_{ST}) show that a sudden increase preceded the storm decrease, thereby cancelling most of the storm onset in the one-hour D_{ST} . This missing current shows up clearly in the ASY component, leading us to believe that a stronger than normal electric field and/or magnetopause compression had distorted the RC, shifted the index from symmetric to asymmetric, and disguised the magnitude of this storm in D_{ST} . Additional support for the nose event identification with a storm injection came from the extensive GGS database.

Examination of WIND data [Ogilvie et al., (1995)] (Figure 3) for April 14 showed that there were several $B_Z < 0$ periods lasting for 1 hour or less. Corresponding CU and CL derived from the CANOPUS array [Rostoker et al., (1995)] show that these periods led to substorms with riometer absorption signatures at auroral latitudes. However the storm trigger appears to be the strong southward turning of $B_Z \sim -10$ nT occurring at 2000 UT, accompanied by a jump in the solar wind speed from 450 km/s to 600 km/s, which produced an even larger B_Z in the compressed magnetic field of the magnetosheath. This period of strong southward B_Z lasted about 3 hours, effectively saturating the ability of the tail to shield out the polar cap potential. The IZMIRAN model [Papitashvili et al., (1994)] predicted in excess of 150 kV across the polar cap for these solar wind conditions.

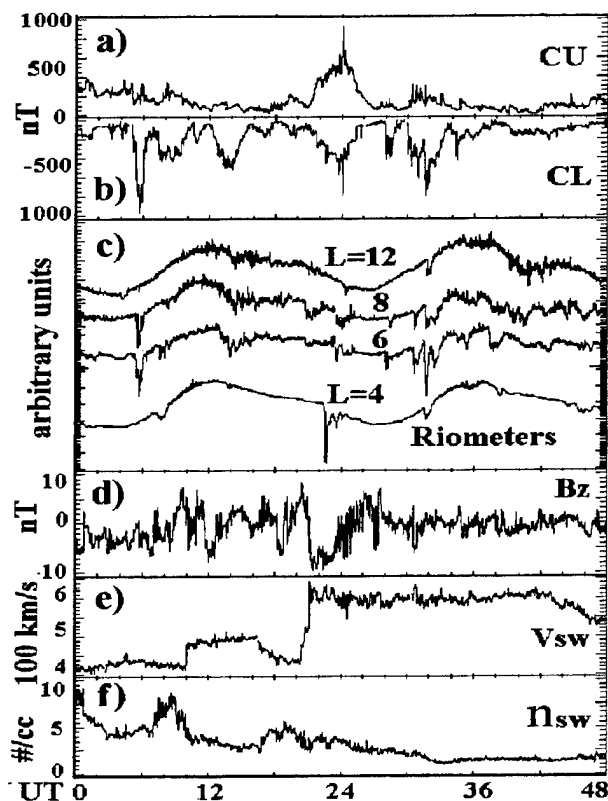


Figure 3. April 14–15, 1996 ISTP data showing: a) CANOPUS CU; b) CL; and c) riometers at $L=12$, 8, 6.6, and 4.4; d) WIND/MFI B_Z component; e) WIND/SWE solar wind velocity; and f) ion density.

The CANOPUS array detected a magnetic bay, a nearly equal response of CU and CL, suggesting that the current systems had moved equatorward, overhead of the magnetometers. Indeed, the Halley Bay magnetometer at $L \sim 4$ [Dudeney et al., (1995)] showed a large H deflection with almost no Z deflection, indicative of strong overhead currents. The ionosphere responded strongly at this time (private communication, J. Aarons, 1996) with enhanced ionospheric scintillations. While CANOPUS riometers at $L > 6$ recorded very little activity, the one at $L=4.4$ as well as Halley Bay, showed an extremely intense and narrow absorption feature at this time, indicating that precipitation had penetrated to low latitudes, deep in the magnetosphere and down to E-layer ionospheric depths.

With complementary ground observations, we surmise that after several intense substorms had pumped up the plasmasheet, a strong convection field injected the plasma to at least $L=4.4$, which POLAR/CEPPAD observed as a 90 keV band. The large

asymmetric component of D_{ST} is evidence that this current was observed by the low latitude stations. The lack of a symmetric D_{ST} response is probably due to the intense but brief (<3 hours) convection electric field associated with this disturbance, which is not enough time to circularize the RC injected in the dusk sector, but not due to the lack of a storm injection *per se*. Thus, despite the contrary magnetometer evidence, we categorize this event with other storm injections as observed on 21 March and 23 October, 1996. We prefer to analyze this injection, however, because both peaks were unusually energetic and well resolved in our instrument, which has an energy threshold of 20 keV.

Field-Aligned Beam

The band of 40 keV field-aligned ions, however, are harder to explain. They have the wrong pitchangles to have convected in from the plasmasheet, because the adiabatic decompression involved in backtracing them to their origin would place them in the plasmasheet loss cone. Nor would ions of this energy have access to the plasmasheet simultaneously with the higher energy, open drift orbit ions, since the magnetosphere is a "notch filter" for only one energy, which implies that these ions are trapped on closed drift orbits. But if they undergo the same processes as the adiabatically energized RC (see Figure 1), which can be seen simultaneously with the banded distribution, they would not be as monoenergetic, nor would they track the energy of the nose ions so precisely. That is, if they had resided for any length of time in the magnetosphere, the same convection that brought in the plasmasheet ions would disperse these ions as well. Nor do the pitchangles, the constant energy, and the L -shell range of these field-aligned ions match the dispersed curves of a substorm injection. Thus we conclude that these field-aligned ions are not convected from some boundary, but *in situ* accelerated during the time of the measurement. This is a key point: no published transport mechanism invoked in storms or substorms can adequately reproduce this feature, which brings us to the hesitant conclusion that these field-aligned ions are energized "in place".

The IPS experiment is a total ion instrument using solid state detectors with a well-known 50 keV "dead" layer for oxygen, so that it cannot respond to the oxygen flux in the field-aligned beam. The POLAR/CAMMICE experiment, however, relies on multi-channel plates and a carbon foil, with a lower, 30 keV threshold for O^+ so that this lower energy

population is observable. Unfortunately CAMMICE was turned off during this period, so we cannot determine the $E > 30$ keV O^+ content for April 15, however when it was switched back on, around April 19, it found an anomalously large amount of O^+ in the RC in two energy bands centered at 40 and 100 keV. Because of the short lifetime of O^+ against charge exchange, such a measurement is consistent with a storm injection at $L=4-7$ occurring only a few days previously, since between storms, CAMMICE detects no O^+ enhancements. A similar storm on March 21 with field-aligned beams showed that the IPS beams are simultaneous in time and energy with the double peaked O^+ spectrum observed by CAMMICE. We also note that POLAR/TIMAS (private communication W. K. Peterson, 1996) did detect $E < 20$ keV O^+ beams on April 15.

Therefore we conclude that on April 15 we are observing H^+ and O^+ ions accelerated to $\sim 30-40$ keV in field-aligned beams, presumably by strong parallel electric fields in the ionosphere. Since these ions track ~ 50 keV below the nose ions, it appears there must be a causal connection, which becomes more apparent when we fit the spectral shape of these populations.

Peak Fits

The three spectral peaks all have differing shape so that we have used three separate functional forms to fit them. Adiabatic energization and diffusion explain the highest energy RC peak, which we are able to fit very well with a Gaussian in $\log(\text{Energy})$ space. The middle "nose" ion peak is represented in our instrument by a response in only one or two channels, which does not constrain the functional form very much. We have chosen to fit this peak with a Gaussian in linear space. The beam reflects a highly asymmetric shape with a long tail toward lowest energies but a sharp cutoff at high energies. After much experimentation, we found that a Chapman layer function, described as $y = a \exp(1 + x - \exp(x))$, where $x \equiv (e - e_1)/\sigma_1$ gave the best fit with the fewest number of free parameters. The 3-peak function was then:

$$Cts = a_1 \exp(1 + x - \exp(x)) + a_2 \exp[(e - e_2)^2 / 2\sigma_2] + a_3 \exp[(\log(e) - \log(e_3))^2 / 2\sigma_3] \quad (1)$$

We have thus fit 16 energy channels with 9 parameters, carrying out this fit for consecutive 96 second averages throughout the nightside pass, Figure 4, where each panel corresponds to a vertical cut through the data of Figure 1b.

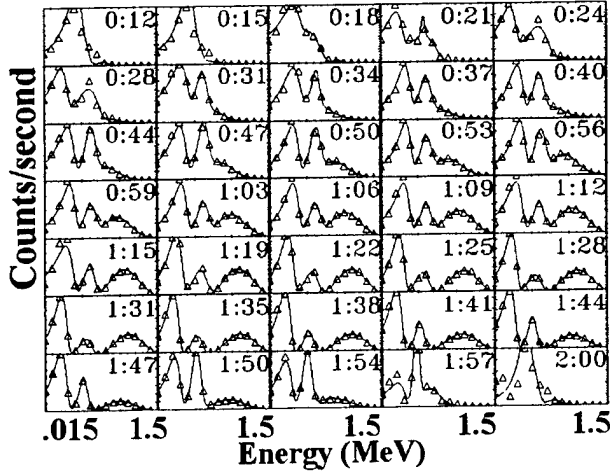


Figure 4. Successive 96s count spectra (symbols) and three peak fit (line) for April 15 data set, corresponding to vertical slices through the data of Figure 1b and Figure 2.

From each panel of the fits in Figure 4, we plot the center energy and the width of the peak to demonstrate how the three populations, beam, nose and RC, evolve during this orbit (Figure 5). The RC is adiabatically energized so that as the model equatorial magnetic field increases the energy increases, as noted by the squares and dashed line. This energization is not seen by the nose ions because they are not an equilibrium trapped population, rather they are a subset of plasmasheet ions that have convective access to this location, such that stronger B-field ions also began with smaller magnetic moment in the magnetotail [Sheldon (1994)].

The 90 keV energy of the nose ions is consistent with a large polar cap potential, though admittedly an asymmetric electric field similar to that observed by CRRES (J. Wygant, unpublished manuscript, 1997) may be necessary to achieve this doubling of the typical nose energy. Most importantly, we find that the ion beam energy, though broader because of the asymmetric shape, tracks the nose energy more precisely when we plot it as a ratio (X) than as a difference (O). This is a most important clue, since the nose energy is completely determined by details of the magnetic topology and convection electric field, whereas the beam appears to be a local, *in situ* phenomenon.

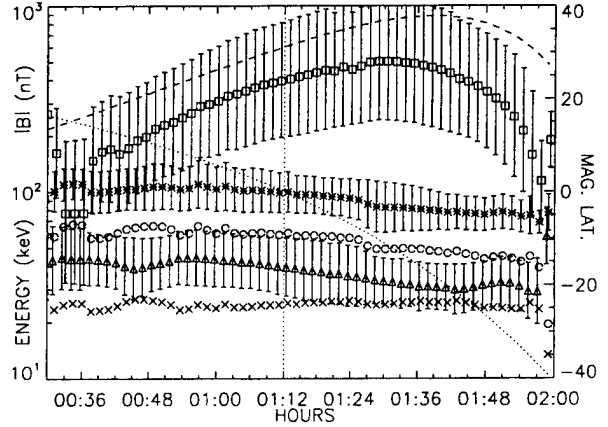


Figure 5. Parameters from the peak fits of Figure 4. Energies of RC (\square), nose ($*$), beam (\triangle), nose - beam (\circ), and the ratio of nose/beam $\times 10$ (\times) are plotted. Error bars are FWHM from peak fits, since fitting errors are negligible. Overplotted dashed line is the model equatorial $|B|$; and the model MLAT (dotted line) linearly scaled from -40 to 40 degrees, with the equator marked with a vertical dotted line.

Discussion and Conclusions

Since these ion beams track the nose ions so closely, we assume that the acceleration process must involve an *in situ* parallel electric field that is somehow related to the energy of the nose ions. Alfvén's pioneering work on parallel electric fields comes to mind [Alfvén and Fälthammer, (1963), Whipple, (1977)] where he argues that one can produce a field-aligned electric field if the electron and ion pitch angle distributions are not identical. Using this event as a guide, a 90 keV monoenergetic nose ion population of ions with equatorial pitch angles less than 90° [Sheldon, (1994)] was superposed on a cold plasmasphere electron population of very different pitch angles. According to Whipple [1977], this would produce a parallel potential drop of several kT_e/e pointing toward the equator. That is, since an ion of pitchangle $\alpha < 90^\circ$ spends most of its time away from the equator, the electrons at the equator will experience a force pulling them toward higher latitudes so as to shield the ion charge, and ions will be repelled toward the equator. This then, is the correct sign of the electric field to account for the ion beams observed by POLAR near the equator. However, there is little evidence for ~ 10 keV electrons, and our data show that the field-aligned beam tracks the energy of the nose ions, not the background electrons. A lengthier treatment of this puzzle will appear in a later paper.

Thus it appears that a parallel electric field is a nat-

ural consequence of storm injections, and may provide an important link in the storm progression. The presence of oxygen in the beam suggests that this parallel field penetrates down to nearly ionospheric depths and may play an important part in the development of D_{ST} during storms. The asymmetric shape of the ion beam spectrum is also suggestive of an extended extraction potential. Could it be that we are observing the magnetospheric signature of a parallel potential structure usually observed only in the auroral zone?

References

- Alfvén, H. and C.-G. Fälthammar. *Cosmical Electrodynamics, Fundamental Principles*. Clarendon, Oxford, 1963.
- Blake, J. B. et al. CEPPAD: Comprehensive energetic particle and pitch angle distribution experiment on POLAR. In C. T. Russell, editor, *The Global Geospace Mission*, pages 531–562. Kluwer Academic Publishers, 1995.
- Dudeney, J. R. et al. Satellite experiments simultaneous with antarctic measurements (SESAME). In C. T. Russell, editor, *The Global Geospace Mission*, pages 705–742. Kluwer Academic Publishers, 1995.
- Fennell, J. F., D. R. Croley, Jr., and S. M. Kaye. Low-energy ion pitch angle distributions in the outer magnetosphere: Ion zipper distributions. *J. Geophys. Res.*, 86, 3375, 1981.
- Ogilvie, K. W. et al. SWE, a comprehensive plasma instrument for the wind spacecraft. In C. T. Russell, editor, *The Global Geospace Mission*, pages 55–77. Kluwer Academic Publishers, 1995.
- Papitashvili, V. O. et al. Electric potential patterns in the northern and southern polar regions parameterized by interplanetary magnetic field. *J. Geophys. Res.*, 99, 13,251, 1994.
- Rostoker, G. et al. Canopus - a ground-based instrument array for remote sensing the high latitude ionosphere during the ISTP/GGS program. In C. T. Russell, editor, *The Global Geospace Mission*, pages 743–760. Kluwer Academic Publishers, 1995.
- Sheldon, R. B. and J. D. Gaffey, Jr. Particle tracing in the magnetosphere: New algorithms and results. *Geophys. Res. Lett.*, 20, 767–770, 1993.
- Sheldon, R. B. Plasmasheet convection into the inner magnetosphere during quiet conditions. In D. N. Baker, editor, *Solar Terrestrial Energy Program: COSPAR Colloquia Series*, volume 5, pages 313–318, New York, 1994. Pergamom Press.
- Smith, P. and R. Hoffman. Direct observations in the dusk hours of the characteristics of the storm time ring current particles during the beginning of magnetic storms. *J. Geophys. Res.*, 79, 966, 1974.
- Whipple, Jr, E. C. The signature of parallel electric fields in a collisionless plasma. *J. Geophys. Res.*, 82, 1525, 1977.

TECHNOLOGY OPERATIONS

The Aerospace Corporation functions as an "architect-engineer" for national security programs, specializing in advanced military space systems. The Corporation's Technology Operations supports the effective and timely development and operation of national security systems through scientific research and the application of advanced technology. Vital to the success of the Corporation is the technical staff's wide-ranging expertise and its ability to stay abreast of new technological developments and program support issues associated with rapidly evolving space systems. Contributing capabilities are provided by these individual Technology Centers:

Electronics Technology Center: Microelectronics, VLSI reliability, failure analysis, solid-state device physics, compound semiconductors, radiation effects, infrared and CCD detector devices, Micro-Electro-Mechanical Systems (MEMS), and data storage and display technologies; lasers and electro-optics, solid state laser design, micro-optics, optical communications, and fiber optic sensors; atomic frequency standards, applied laser spectroscopy, laser chemistry, atmospheric propagation and beam control, LIDAR/LADAR remote sensing; solar cell and array testing and evaluation, battery electrochemistry, battery testing and evaluation.

Mechanics and Materials Technology Center: Evaluation and characterization of new materials: metals, alloys, ceramics, polymers and composites; development and analysis of advanced materials processing and deposition techniques; nondestructive evaluation, component failure analysis and reliability; fracture mechanics and stress corrosion; analysis and evaluation of materials at cryogenic and elevated temperatures; launch vehicle fluid mechanics, heat transfer and flight dynamics; aerothermodynamics; chemical and electric propulsion; environmental chemistry; combustion processes; spacecraft structural mechanics, space environment effects on materials, hardening and vulnerability assessment; contamination, thermal and structural control; lubrication and surface phenomena; microengineering technology and microinstrument development.

Space and Environment Technology Center: Magnetospheric, auroral and cosmic ray physics, wave-particle interactions, magnetospheric plasma waves; atmospheric and ionospheric physics, density and composition of the upper atmosphere, remote sensing, hyperspectral imagery; solar physics, infrared astronomy, infrared signature analysis; effects of solar activity, magnetic storms and nuclear explosions on the earth's atmosphere, ionosphere and magnetosphere; effects of electromagnetic and particulate radiations on space systems; component testing, space instrumentation; environmental monitoring, trace detection; atmospheric chemical reactions, atmospheric optics, light scattering, state-specific chemical reactions and radiative signatures of missile plumes, and sensor out-of-field-of-view rejection.